PHYSICAL AND REDUCED-ORDER DYNAMIC ANALYSIS OF MEMS

S. K. De and N. R. Aluru

Beckman Institute for Advanced Science and Technology
University of Illinois at Urbana-Champaign
405 N. Mathews Avenue, Urbana, IL 61801

ABSTRACT

In this paper, we first present an efficient physical level simulation method for the dynamic analysis of electrostatic micro-electro-mechanical systems (MEMS). This method is then used to analyze MEMS dynamics. Stiffness hardening or softening of MEM structures has been shown to depend both on the applied voltage and the geometry. The existence of multiple resonant peaks in the frequency response diagram has been presented. We have shown that a DC bias along with an appropriate AC bias can give fast switching at a considerably less peak power requirement. Finally, a reduced order model has been developed based on Karhunen-Loève decomposition for the dynamic simulation of MEMS. Reduced order models are cheap in terms of memory and computational time and are needed to perform fast and efficient system-level composite circuit and micro-mechanical simulations.

keywords: MEMS, dynamics, resonant frequency, switching speed and power, reduced order modeling.

1. INTRODUCTION

The coupled electrical-mechanical nature of electrostatic MEMS [1] gives rise to interesting dynamic characteristics of these devices which can have significant impact in their applications as capacitive switches, resonators, tunable capacitors, inductors and filters [2]. In this paper, we first develop an efficient physical level simulation method for the dynamics analysis of MEMS and then analyze the two important MEM dynamic parameters, namely, resonant frequency and switching speed. Resonant frequency of the MEM device is an important parameter as it indirectly affects design parameters like Q-factor, the switching speed of the device and effects of external noise. Switching speed is a major limitation of capacitive switches with respect to their applications in radar systems and wireless communications. Experimental and analytical works [3] have shown the bending of the frequency response curve of MEM devices with increasing/decreasing voltages in the context of resonant frequency studies. In this paper, we show that resonant frequency can both decrease as well as increase with increasing applied voltage, depending on the geometry of the device. Most importantly, the existence of multiple peaks in the frequency response curves have been presented, which can be a important design concern. It has been shown that faster switching can be achieved for capacitive switches at a considerably less peak power requirement by using a AC signal at half of the resonant frequency of the structure along with a DC bias.

Low order dynamic models based on Karhunen-Loève (KL) method have been developed in [4], [5]. However, these models are based on the one-dimensional beam equation and analytical

expression of the electrostatic force. In this paper, we present a reduced order model based on KL decomposition, 2D linear elasticity and a boundary integral formulation of the electrostatic force. It does not use any analytical expressions and as a result is very general in nature.

2. PHYSICAL LEVEL SIMULATION

Physical level analysis of electrostatic MEMS dynamics requires a self-consistent solution of the coupled mechanical and electrical equations at each time step. Figure 1 shows a typical MEM device, a deformable cantilever beam over a fixed ground plane. At a given time instant (starting point of a time step), the applied voltage between the cantilever beam and the ground plane induces electrostatic charges distributed on the surface of the conductors. These charges give rise to electrostatic forces, which act normal to
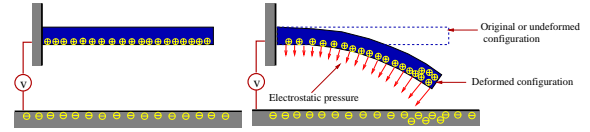

Figure 1: A cantilever beam over a ground plane (a) applied voltage causes a charge distribution (b) the deformed structure with charge redistribution

the surface of the conductors and deforms the cantilever beam further from its initial position. When the beam deforms, the charge redistributes on the surface of the conductors and, consequently, the resultant electrostatic forces and the deformation of the beam also change. This process continues until a self-consistent final state is reached for that time step.

2.1. Governing Equations and Algorithm

The mechanical deformation of the MEM structure due to the electrostatic forces is obtained by performing 2-D geometrically non-linear analysis of the micro-structure. The transient governing equations for an elastic body using a Lagrangian description are given by [6]

$$\rho\ddot{\mathbf{u}} + c\dot{\mathbf{u}} = \nabla \cdot (\mathbf{FS}) \qquad in \quad \Omega \qquad (1)$$

$$\mathbf{u} = \mathbf{G} \qquad on \quad \Gamma_g \qquad (2)$$

$$\mathbf{P} \cdot \mathbf{N} = \mathbf{H} \qquad on \quad \Gamma_h \qquad (3)$$

$$\mathbf{u}|_{t=0} = \mathbf{G_0} \qquad in \quad \Omega \qquad (4)$$

$$\dot{\mathbf{u}}|_{t=0} = \mathbf{V_0} \qquad in \quad \Omega \qquad (5)$$

where ρ and c are the material density and material damping factor. $\mathbf{F}$ is the deformation gradient, $\mathbf{u}$, $\dot{\mathbf{u}}$ and $\ddot{\mathbf{u}}$ are the displacement, velocity and acceleration vectors, respectively, $\mathbf{N}$ is the unit outward normal vector in the initial configuration, $\mathbf{S}$ is the second Piola-Kirchhoff stress, $\mathbf{G}$ is the prescribed displacement, $\mathbf{G_0}$ and $\mathbf{V_0}$ are the initial displacement and velocity, respectively, $\mathbf{H}$ is the electrostatic pressure acting on the surface of the structures and $\mathbf{P}$ is the first Piola-Kirchhoff stress tensor. A Newmark scheme [7] with an implicit trapezoidal rule is used for solving the dynamic problem of the nonlinear elastic domain. Numerical discretization is done using the Finite Cloud Method (see [8] for details).

The 2D governing equation for electrostatic analysis can be written in a Lagrangian boundary integral form as [9]

$$\phi(p(P)) = \int_{d\Omega} \frac{1}{\varepsilon} G(p(P), q(Q))\sigma(q(Q))\mathbf{J}(Q)d\Gamma_Q + C \quad (6)$$

$$\int_{d\Omega} \sigma(q(Q))\mathbf{J}(Q)d\Gamma_Q = C_T \quad (7)$$

$$\mathbf{J}(Q) = [\mathbf{T}(Q) \cdot \mathbf{C}(Q)\mathbf{T}(Q)]^{\frac{1}{2}} \quad (8)$$

where ε is the dielectric constant of the medium, P and Q are the source and field points in the initial configuration corresponding to the source and field points p and q in the deformed configuration and G is the Green's function. In two dimensions, $G(p,q) = -ln|p-q|/2\pi$, where $|p-q|$ is the distance between the source point p and the field point q. C_T is the total charge of the system and C is an unknown variable which can be used to compute the potential at infinity. $\mathbf{T}(Q)$ is the tangential unit vector at field point Q and $\mathbf{C}(Q)$ is the Green deformation tensor. The need to update the geometry of the structures in the conventional approach presents several difficulties (see [9] for details) and has been eliminated by the Lagrangian representation. The electro-

---

Algorithm 1 A procedure for self-consistent dynamic analysis of coupled electromechanical devices by using a Lagrangian approach for both mechanical and electrostatic analysis

1. Initialize $\mathbf{u} = \mathbf{u}^0$ and $\dot{\mathbf{u}} = \dot{\mathbf{u}}^0$
2. Compute $\nabla \cdot (\mathbf{FS})^0$, $[\mathbf{F}^0 = \mathbf{F}(\mathbf{u}^0), \mathbf{S}^0 = \mathbf{S}(\mathbf{u}^0)]$
3. Compute $\ddot{\mathbf{u}}$ - Eqn. (1)
4. Begin a time step
repeat
   a. Compute $\mathbf{T}(Q)$ and $\mathbf{C}(Q)$ from $\mathbf{u}$
   a. Compute $\mathbf{J}(Q)$ - Eqn. (8)
   b. Do electrostatic analysis on undeformed geometry for $\mathbf{J}(Q)$ to compute surface charge density - Eqns. (6-7)
   c. Compute electrostatic pressure $\mathbf{H}$.
   e. Do mechanical analysis on undeformed geometry to compute structural displacements $\mathbf{u}$ - Eqns. (1-5)
until a self-consistent final stage is reached
5. Update $\ddot{\mathbf{u}}$ and $\dot{\mathbf{u}}$
6. End of a time step
7. Repeat 4-6 for all time steps

---

static pressure can be computed from the surface charge density by the relation $\mathbf{H} = P_e J\mathbf{F}^{-T}\mathbf{N}$ where P_e is the electrostatic pressure normal to the surface given by $P_e = \frac{\sigma^2}{2\varepsilon}$ and $J = det(\mathbf{F})$. Boundary Cloud Method is used for the numerical discretization of the electrostatic boundary integral equations (see [9] for details). The various steps for solving the governing equations to do a dynamic analysis of MEM devices is given in Algorithm 1.

3. RESULTS AND ANALYSIS OF MEMS DYNAMICS

Figure 2 shows the dynamic pull-in of an undamped ($c = 0$) Si cantilever beam ($80\mu m$ long, $10\mu m$ wide and $0.5\mu m$ thick) with an initial gap between the beam and the ground electrode $0.7\mu m$. The Young's modulus is $169GPa$, mass density of $2231kg/m^3$ and Poisson's ratio of 0.3. A time step of $0.1\mu s$ was used. The dynamic pull-in voltage was found to be 2.12V which matches very well with the reported data in [10] based on linear elasticity.
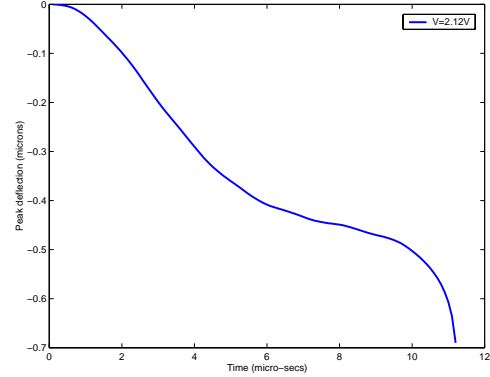

Figure 2: Dynamic pull-in analysis of a cantilever beam.

Proper understanding of the dynamic characteristics of electrostatic MEMS is of utmost importance for the design of electrostatic MEMS based devices. Based on literature study [2], the four main MEMS dynamic parameters are namely - resonant frequency, switching speed, Q-factor and phase shift. In this paper, we analyze the two most important parameters - resonant frequency and switching speed.

3.1. Resonant Frequency

Figure 3 shows the variation in the resonant frequency with the applied voltage for a $80\mu m$ by $10\mu m$ by $0.5\mu m$ fixed-fixed beam for different gaps. The resonant frequency of the MEM structure changes with the applied voltage as the electrical forces act like a non-linear negative spring. Generally, the resonant frequency decreases with the increase in the applied voltage due to "spring-softening" of the beam by the electrical forces as seen for the case with a gap of $0.7\mu m$. However, when non-linearity comes in (due to large deformation), the resonant frequency is found to increase for the fixed-fixed beam cases with gaps $2.0\mu m$ and $4.0\mu m$. In these cases, the spring-hardening effect due to mechanical forces is larger than the spring-softening effect of the electrical forces.

Figure 4 show the frequency response curve of a $80\mu m$ by $10\mu m$ by $1.0\mu m$ fixed-fixed beam with a gap of $0.7\mu m$ with a material damping factor $c = 2\rho$ for different voltages. From Figure 4 it can be seen that as the AC peak voltage is increased, the nature of the frequency response curve changes. Two peaks in the amplitude occur instead of a single peak. The primary peak occurs near the resonant frequency of the beam which is around $1300KHz$ due to the constant DC voltage. The AC component of the signal gives rise to the secondary peak. Since the electrostatic force may be regarded as proportional to the square of the voltage V^2, a resonance is expected near $\frac{1}{2}f_{res}$ where f_{res} is the resonant frequency and that matches with the secondary peak which is at
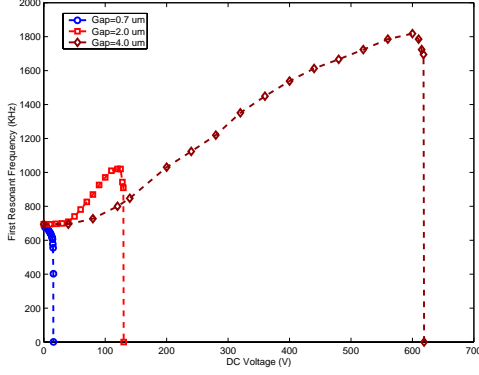
Figure 3: Resonant Frequency vs Voltage for a fixed-fixed beam for different gaps.

roughly $650KHz$. The existence of multiple resonant peaks in the frequency response curves can be a important design concern as the application of frequencies near resonant frequencies are often unstable states of the device.
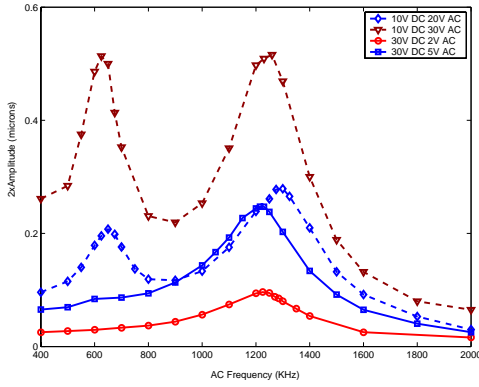

Figure 4: Frequency response curves for different DC bias and AC signals.

3.2. Switching Speed

Switching can be of two types in electrostatic MEMS- switch down and switch up. Switch down is equivalent to pull-in in electrostatic MEM switches. The time taken by the switch to pull-in under an applied voltage is called switch down time. For switch-down under a DC or an AC signal, the switching speed increase with the increase in the applied voltage as larger voltage gives rise to larger electrostatic force which in turn gives rise to larger acceleration and hence faster pull-in [11] . Our simulations further show that as the frequency of an applied AC signal nears half of the resonant frequency ($650KHz$), the switching speed increases and it can be used to enhance switching speed. Operating near resonant frequency in the case of switch-down is acceptable as the structure does not vibrate but just collapses as shown in Figures 2.

The generalized circuit for the MEM device consists of a power source (applied voltage V), a capacitor (the switch) and a resistance (the Silicon beam acting as the capacitive switch) in series.

The capacitance C and the resistance R of the beam can easily calculated for both deformed/undeformed states [12] . The governing equation for the MEM circuit is [12]

$$V = V_C + V_R = v + Ri = v + R\frac{dq}{dt} = v + R[C\frac{dv}{dt} + v\frac{dC}{dt}] \quad (9)$$

where V_C or v is the voltage drop across the capacitive switch and V_R is the voltage drop across the resistance. i is the current, q is the charge on the capacitor and t is time. The power (P) consumed at any instant of time is given by $P = Vi$. Equation (9) is solved numerically at each time instant and the instantaneous power computed during the dynamic simulations. Figure 5 shows the peak power consumption for different signals and switching times for the undamped $80\mu m$ by $10\mu m$ by $1.0\mu m$ fixed-fixed beam with a gap of $0.7\mu m$. It can be seen that a AC signal with a frequency close to half of the resonant frequency and a DC bias gives faster switching at a considerably less (almost 40 percent) peak power requirement than a pure DC bias. Resonance plays a key role in this reduction of peak power consumption.
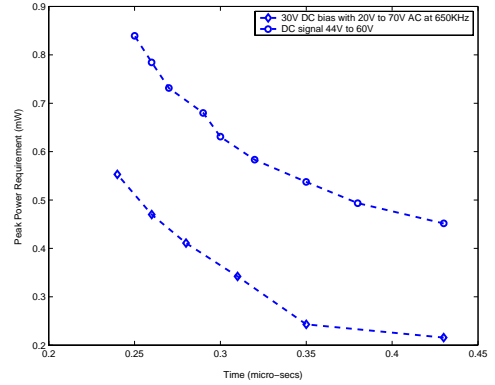

Figure 5: Peak Power requirement for various signal types.

4. REDUCED ORDER MODELING IN MEMS DYNAMICS

An efficient reduced order model (ROM) has been developed for simulating MEMS dynamics based on KL decomposition. Physical level simulation becomes very expensive and impractical for repeated simulation of complex MEM devices needed in any design process. ROMs are also needed to perform fast and efficient system-level composite circuit and micro-mechanical simulations.

4.1. Basis Generation

The key idea in a ROM model is to express the unknowns in terms of a few global basis functions. For the dynamic simulation of MEM devices, the unknowns are the x and y displacements and surface charge density (which gives rise to the electrostatic pressure). The global functions are generated from snapshots taken from a few full simulations of the dynamics. For our method, the displacement basis functions are generated from the full simulation of just linear dynamics of the beam. 50 snapshots (n_s) are taken from the linear dynamic simulation of the undamped $80\mu m$ by $10\mu m$ by $1.0\mu m$ fixed-fixed beam for an applied pressure of

$500KPa$ at the bottom surface. Since the snapshots need to satisfy homogeneous boundary conditions [13] , the steady state $\mathbf{S}(x,y)$ for the applied pressure is removed from the snapshots $\mathbf{U}(x,y,t)$ to get $\mathbf{U_t}(x,y,t)$

$$\mathbf{U_t}(x,y,t) = \mathbf{U}(x,y,t) - \mathbf{S}(x,y). \qquad (10)$$

Here, $\mathbf{U}(x,y,t)$ is either the x or the y-displacements. It has been proved in [4] that the basis functions ($a_i(x,y)$) are simply the column vectors of the matrix $\mathbf{L}$ which is obtained by doing a singular value decomposition (SVD) of the snapshots ensemble matrix $\widetilde{\mathbf{U_t}}$

$$\left[\widetilde{\mathbf{U_t}}\right] = \mathbf{LAR^T} \qquad (11)$$

where $\widetilde{\mathbf{U_t}}$ is the matrix containing the snapshot informations:

$$\left[\widetilde{\mathbf{U_t}}\right] = [\mathbf{U_t}(x,y,t_1), \mathbf{U_t}(x,y,t_2), ..., \mathbf{U_t}(x,y,t_{ns})] \qquad (12)$$

The basis functions for the charge density are obtained by the dynamic simulation of the considered fixed-fixed beam with a gap of $0.7\mu m$ for a 20V DC signal. For the boundary integral equation, there are no non-homogeneous boundary conditions and we do not subtract any steady part. Other than that, the electrical basis ($b_i(x,y)$) is generated in the same manner as the mechanical basis ($a_i(x,y)$) using Equation (11) where $\mathbf{U_t}(x,y,t)$ is the ensemble of snapshots of charge densities instead of displacement now.

4.2. Results of Reduced Order Models

Using the basis functions generated in section 4.1, we simulate the dynamics of the same device. The unknowns are expressed as a linear combination of global basis functions and a multiple of the steady state in case of the displacements, i.e.,

$$\mathbf{D}(x,y,t) = \sum_{i=1}^{q} \alpha_i(t) a_i(x,y) + k\mathbf{S}(x,y) \qquad (13)$$

$$\mathbf{E}(x,y,t) = \sum_{i=1}^{r} \beta_i(t) b_i(x,y) \qquad (14)$$

where $\mathbf{D}(x,y,t)$ is the x or y displacement and $\mathbf{E}(x,y,t)$ is the surface charge density. a_i and b_i are vectors denoting the ith global basis function for displacement and surface charge density. q and r are the number of mechanical and electrical basis functions used, $k = \frac{P(t)}{P_0}$ is the ratio of the applied pressure at an time instant to the pressure used to generate the mechanical basis. α_i and β_i are the unknown parameters that need to be determined at a time instant. The derivatives of the unknowns are expressed in terms of the derivatives of the basis function vectors a_i and b_i. We use collocation (i.e., satisfy the governing equations at each point in the domain) and the overdetermined system is solved by the method of normal equations. Figure 6 compares the displacement at the center of the fixed-fixed beam given by the ROM with full simulation for a 10V DC signal. We can see that for small deformation, linear analysis is exact and hence can be effectively used as it is much faster than non-linear analysis. The ROM simulations match pretty well with the full simulations and it is found that 3 electrical and mechanical basis functions are more than sufficient for efficiently capturing the process. The simulation time for the ROM was half of the full simulation time. As we go to complex devices, the difference will be more significant.
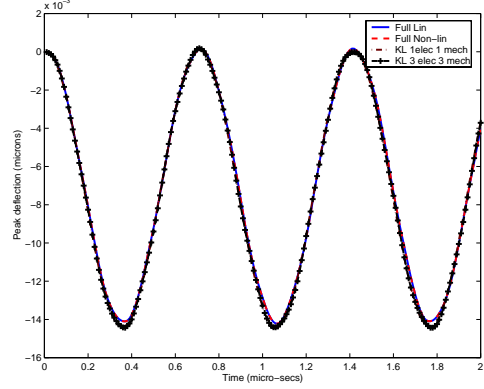

Figure 6: ROM vs full simulation for 10V DC signal.

5. CONCLUSIONS

We have presented an efficient physical level simulation method for the dynamic simulation of MEMS. The hardening and the softening phenomena of the MEM devices has been found to depend both on the applied electric field and geometry. The frequency response curves of MEM devices can exhibit multiple peaks depending on the applied voltage and can be a important design concern. Fast switching at low power can be achieved by a DC biased AC signal close to the half of resonant frequency. A ROM has been developed for MEM dynamics simulations based on KL decomposition which can be efficiently used for repeated simulations of a MEM device.

6. REFERENCES

[1] N. R. Aluru and J. White, *Sensors and Actuators A*, 58, 1-11, 1997.

[2] J. M. Huang, K. M. Liew, C. H. Wong, S. Rajendran, M. J. Tan and A. Q. Liu, *Sensors and Actuators A*, 93, 273-285, 2001.

[3] C. Gui, R. Legtenberg, H. A. Tilmans, J. H. Fluitman and M. Elwenspoek, *J. of MEMS*, 7, 122-127, 1998.

[4] E. S. Hung and S. D. Senturia, *J. of MEMS*, 8(3), 280-289, 1999.

[5] Y. C. Liang, W. Z. Lin, H. P. Lee, S. P. Kim. K. H. Lee and H. Sun, *J. of Sound and Vibs.*, 256(3), 515-532, 2002.

[6] D. S. Chandrasekharaiah and L. Debnath, Continuum Mechanics, Academic Press, 1994.

[7] K. J. Bathe, Finite Element Procedures, Prentice-Hall, 1995.

[8] X. Jin, G. Li and N. R. Aluru, *CMES*, 2(4), 447-462, 2001.

[9] G. Li and N. R. Aluru, *J. of MEMS*, 11(3), 245-254, 2002.

[10] N. R. Aluru, *Computational Mechanics*, 23, 324-338, 1999.

[11] G. K. Ananthasuresh, R. K. Gupta and S. D. Senturia, *MEMS, ASME Dynamic Systems and Control (DSC) Series*, 59, 401-407, 1996.

[12] E. Hughes, Hughes Electrical Technology, Longman Scientific Technical, 1987.

[13] H. M. Park, M. W. Lee, *Comput. Methods Appl. Mech. Engrg.*, 188, 165-186, 2000.